Effects of Lipid Composition on Membrane Permeabilization by Sticholysin I and II, Two Cytolysins of the Sea Anemone *Stichodactyla helianthus*

Carlos Alvarez Valcarcel,*† Mauro Dalla Serra,* Cristina Potrich,* Ivonne Bernhart,* Mayra Tejuca,† Diana Martinez,† Fabiola Pazos,† Maria E. Lanio,† and Gianfranco Menestrina*

*CNR-ITC, Centro di Fisica degli Stati Aggregati, I-38050 Povo, Italy, and †Departamento de Bioquimica, Facultad de Biologia, Universidad de la Habana, La Habana, Cuba

ABSTRACT Sticholysin I and II (St I and St II), two basic cytolysins purified from the Caribbean sea anemone *Stichodactyla helianthus*, efficiently permeabilize lipid vesicles by forming pores in their membranes. A general characteristic of these toxins is their preference for membranes containing sphingomyelin (SM). As a consequence, vesicles formed by equimolar mixtures of SM with phosphatidylcholine (PC) are very good targets for St I and II. To better characterize the lipid dependence of the cytolysin-membrane interaction, we have now evaluated the effect of including different lipids in the composition of the vesicles. We observed that at low doses of either St I or St II vesicles composed of SM and phosphatidic acid (PA) were permeabilized faster and to a higher extent than vesicles of PC and SM. As in the case of PC/SM mixtures, permeabilization was optimal when the molar ratio of PA/SM was ~1. The preference for membranes containing PA was confirmed by inhibition experiments in which the hemolytic activity of St I was diminished by pre-incubation with vesicles of different composition. The inclusion of even small proportions of PA into PC/SM LUVs led to a marked increase in calcein release caused by both St I and St II, reaching maximal effect at ~5 mol % of PA. Inclusion of other negatively charged lipids (phosphatidylserine (PS), phosphatidylglycerol (PG), phosphatidylinositol (PI), or cardiolipin (CL)), all at 5 mol %, also elicited an increase in calcein release, the potency being in the order CL $\approx$ PA $\gg$ PG $\approx$ PI $\approx$ PS. However, some boosting effect was also obtained, including the zwitterionic lipid phosphatidylethanolamine (PE) or even, albeit to a lesser extent, the positively charged lipid stearylamine (SA). This indicated that the effect was not mediated by electrostatic interactions between the cytolysin and the negative surface of the vesicles. In fact, increasing the ionic strength of the medium had only a small inhibitory effect on the interaction, but this was actually larger with uncharged vesicles than with negatively charged vesicles. A study of the fluidity of the different vesicles, probed by the environment-sensitive fluorescent dye diphenylhexatriene (DPH), showed that toxin activity was also not correlated to the average membrane fluidity. It is suggested that the insertion of the toxin channel could imply the formation in the bilayer of a nonlamellar structure, a toroidal lipid pore. In this case, the presence of lipids favoring a nonlamellar phase, in particular PA and CL, strong inducers of negative curvature in the bilayer, could help in the formation of the pore. This possibility is confirmed by the fact that the formation of toxin pores strongly promotes the rate of transbilayer movement of lipid molecules, which indicates local disruption of the lamellar structure.

INTRODUCTION

Sticholysin I and II (St I and St II) are the two most potent cytolysins purified from the Caribbean sea anemone *Stichodactyla helianthus* (order Actiniaria). They belong to a group of highly homologous proteins, characterized by high pI, molecular size ~20 kDa, inhibition by sphingomyelin (Bernheimer, 1990; Kem, 1988; Macek et al., 1994; Turk, 1991) and predominant β structure (Menestrina et al., 1999), collectively called actinoporins (Kem, 1988). St I and St II together constitute >90% of the cytolytic fraction of the anemone venom (Lanio et al., 2001). They are characterized by a few amino acid substitutions, 13, scattered throughout the primary sequence, which could in principle originate a different mechanism of action. Indeed, a different lipid dependence has been reported for St I (Tejuca et al., 1996) and St II (De Los Rios et al., 1998). In addition, the hemolytic activity of St II is higher than that of St I, 30,000 HU/mg and 21,700 HU/mg, respectively (Lanio et al., 2001). Both St I and St II, as well as probably all other actinoporins, exert their cytolytic action by forming oligomeric pores in the cell membrane (De Los Rios et al., 1998; Tejuca et al., 1996), and therefore belong to the large protein superfamily of pore-forming toxins (PFT).

The interest in these toxins has risen in recent years. Besides being important envenoming and pathogenic factors, studied to understand their mode of action, PFT are also useful for clarifying basic mechanisms such as polypeptide insertion into membranes, self-aggregation, pore assembly, and solute permeation through the newly formed pores (Lacy and Stevens, 1998; Lesieur et al., 1997). In addition, they are increasingly recognized as attractive tools for biotechnological and pharmaceutical applications. They have been used for the construction of antitumoral or antimicrobial toxins (Al-yahyaee and Ellar, 1996; Panchal et al., 1996; Pederzolli et al., 1995; Tejuca et al., 1999), for the selective permeabilization of mammalian cells, allowing the investigation of diverse cell functions (Ahnert-Hilger

Received for publication 3 August 2000 and in final form 28 February 2001.

Address reprint requests to Gianfranco Menestrina, CNR Centro di Fisica degli Stati Aggregati, Via Sommarive 18, I-38050 Povo (TN), Italy. Tel.: 39-0461-314256; Fax: 39-0461-810628; E-mail: menes@cefsa.itc.it

0006-3495/01/06/2761/14 $2.00

and Weller, 1997; Bhakdi et al., 1993) or the loading of foreign molecules (Russo et al., 1997) and, finally, for the creation of switchable pores that open and close at the application of different stimuli (Bayley, 1995; Gu et al., 1999). From this point of view, eukaryotic actinoporins constitute an interesting alternative to the most studied prokaryotic PFT, though their molecular mechanism of action is still less well understood.

Actinoporins are very potent toxins affecting almost all kind of eukaryotic cells on which they have been tried (Macek et al., 1994). The reason for this apparent nonselectivity is that they use sphingomyelin, a lipid that is ubiquitous in animal cells, as a low-affinity acceptor (Macek et al., 1995). Exploiting as acceptors certain diffuse classes of lipids is indeed a common feature in the PFT family. Examples are cholesterol binding bacterial cytolysins (Alouf and Geoffroy, 1991), the sphingomyelin (SM)-seeking hemolytic lectin CEL-III of the sea cucumber (Hatakeyama et al., 1999), and *Vibrio* cytolysins requiring both cholesterol and SM (Bhakdi et al., 1993). Besides being always present, these fundamental components of the animal cell membrane are particularly enriched in specialized micro-regions, called lipid rafts (Edidin, 1997; Rietveld and Simons, 1998), and this may help the toxin reaching in those regions a critical concentration necessary for aggregation and pore formation (Fivaz et al., 1999). In addition to major components, such as phosphatidylcholine (PC), SM, and cholesterol, cell membranes contain many other lipids, albeit in lower amounts. Making use of the ability of actinoporins to permeabilize model membranes, such as lipid vesicles, we decided to investigate the role of lipid composition in this interaction. Permeabilizing effects by St I and St II were compared to other properties of the different vesicles prepared, such as size, polydispersity, and fluidity. Results suggest an important role played by even minor amounts of phosphatidic acid and cardiolipin, two lipids inducing negative curvature in bilayers, and suggest that the tendency of these lipids to induce negative curvature of the bilayer could be involved in the mechanism of pore formation.

MATERIALS AND METHODS

Reagents

St I and St II were purified as described (Alvarez et al., 1998; Lanio et al., 2001) by combining gel filtration chromatography on Sephadex G-50 medium (Amersham-Pharmacia Biotech, Uppsala, Sweden) and ionic exchange chromatography on CM-cellulose 52 (Whatman, Maidstone, UK). Calcein was obtained through Sigma Chemical Co. (Milan, Italy) and Triton X-100 (Tx100) from Merck (Milan, Italy). Lipids used were egg phosphatidylcholine (PC), phosphatidylserine (PS), phosphatidic acid (PA), phosphatidylglycerol (PG), phosphatidylinositol (PI), cardiolipin (CL), sphingomyelin (SM), phosphatidylethanolamine (PE), stearylamine (SA), and 1-palmitoyl-2-[6-[(7-nitrobenz-2-oxa-1,3-diazol-4-yl)amino]caproyl]-*sn*-glycero-3-phosphocholine (P-C6-NBD-PC). All lipids were purchased from Avanti Polar Lipids (Alabaster, AL), and were >99% pure as stated by the purchaser.

Preparation of lipid vesicles

Small unilamellar vesicles (SUV) were prepared by thorough sonication of a multilamellar liposomes suspension in 10 mM Tris-HCl, pH 7.4, as described earlier (Pazos et al., 1998). Large unilamellar vesicles (LUVs) were prepared as already described (Tejuca et al., 1996) by extruding a solution of multilamellar liposomes prepared in the presence of 80 mM calcein (pH 7.0 adjusted by NaOH), and subjected to six cycles of freezing and thawing. A two-syringe extruder was used, equipped with two stacked polycarbonate filters (Nuclepore, Maidstone, UK) with 100-mm holes (MacDonald et al., 1991). Thirty-one passages were performed each time. Lipid compositions used are reported in the text. The initial lipid concentration, either with SUV or LUV, was 10 mg/ml. To remove untrapped calcein, the vesicles were spun through mini-columns (Pierce, Rockford, IL) loaded with Sephadex G-50 (medium) pre-equilibrated with 100 mM NaCl, 1 mM EDTA, and 10 mM Tris-HCl, pH 7.4 (elution buffer).

Inhibition of the hemolytic activity of St I

SUV were used for the hemolytic activity inhibition experiments. SUV of SM, PC/SM (1:1), SM/PA (1:1), or PC were incubated with sticholysins at different lipid/toxin molar ratio, as indicated in the text, and the remaining hemolytic activity was assayed by measuring the decrease in the turbidity of a human red blood cell (HRBC) suspension measured at 420 nm in a microplate reader (EMS reader NF, version 2.4). Human red blood cells were prepared from pooled fresh human total blood obtained from healthy volunteers as already described (Tejuca et al., 1996).

Vesicle permeabilization

This was determined by measuring the fluorescence of released calcein with a fluorescence microplate reader (Fluostar from SLT, Austria). Fluorescence was excited through a narrow band interference filter centered at 485 nm and was detected after a second filter at 538 nm. White plastic 96-well microplates (Labsystems Fluoroplate, Helsinki, Finland) were pretreated with 0.1 mg/ml Prionex (Pentapharm, Switzerland) which strongly reduces unspecific binding of protein and vesicles to plastic (Dalla Serra et al., 1999). Each well was filled with the elution buffer plus the desired amount of LUV (between 1 and 5 μM depending on lipid composition). Finally, toxin was added, in a total volume of 200 μl, at the concentration reported in the text. After mixing vesicles and toxin, the release of calcein produced an increase in fluorescence, F (due to the dequenching of the dye into the external medium) which was resolved in time. Each reported value is the average of five consecutive readings of the same well (taken at room temperature in 0.5 s). Spontaneous leakage of calcein was negligible under these conditions. Maximum release was always obtained by adding 1 mM Tx100 (final concentration) and provided the fluorescence value F_{max}. The percentage of release R(%) was calculated as follows:

$$R(\%) = (F_{fin} - F_{in})/(F_{max} - F_{in}) \times 100 \qquad (1)$$

where F_{in} and F_{fin} represent the initial and the final (steady-state) value of fluorescence before and after toxin addition.

In the experiments with variable ionic strength the buffer composition was as follows: x · 626 mM NaCl, $(1 - x)$ · 1252 mM sucrose, 1 mM EDTA, and 10 mM Tris-HCl, pH 7.4, with x ranging from one to zero. In this way the osmolarity of the solution was kept constant while varying the ionic strength. Vesicles were pre-equilibrated in this solution for at least 15 min before adding the toxin.

Fluorescence polarization measurements

Diphenylhexatriene (DPH) fluorescence polarization measurements were carried out in a photon counting spectrofluorimeter (Spex Fluoromax,

Edison, NJ) using excitation wavelength 358 nm (5-nm slit) and emission wavelength 427 nm (5-nm slit). Polarization (P) was measured using two Glan-Thompson quartz polarizers and was determined as follows (Lakowicz, 1983):

$$P = (I_{vv} - G \cdot I_{vh})/(I_{vv} + G \cdot I_{vh}) \quad (2)$$

$$G = I_{hv}/I_{hh} \quad (3)$$

where I is the observed fluorescence intensity and the first of the two subscripts refers to the position of the excitation polarizer, the second to that of the emission polarizer, v stands for vertical, and h for horizontal (defined with respect to the optical plane). G is a correction factor introduced to compensate for the different optical transmission of the apparatus with vertically and horizontally polarized light (Lakowicz, 1983). Measured G was typically 1.06 ± 0.01. DPH was diluted at 50 nM in elution buffer from a concentrated stock solution and vesicles were added at a final lipid concentration of 20 μM.

Measurement of vesicles size by photon correlation spectroscopy

LUV size was determined by photon correlation spectroscopy (as in Mayer et al., 1986) at a fixed angle (90°) and room temperature, using a laser particle sizer (Malvern Z-sizer 3, Malvern, UK) equipped with a 5-mW He-Ne laser. Lipid concentration was in the range between 2 and 20 μg/ml. A 64-channel correlator was used which can provide particle size estimates in the range from 5 to 5000 nm. Data were analyzed by the cumulant method using Malvern Application Software. The first cumulant provides the apparent diffusion coefficient of the vesicles from which the hydrodynamic radius ⟨R⟩ can be derived through the Stokes-Einstein relation (Pecora, 1985; Santos and Castanho, 1996). Distribution width was calculated from the second cumulant, as reported in (Santos and Castanho, 1996).

Determination of the rate of lipid flip-flop in vesicles

The transbilayer movement of a short-chain fluorescent lipid, P-C6-NBD-PC, was measured by mixing labeled LUVs with bovine serum albumin (BSA). Selective extraction of the labeled lipid by BSA was detected via the decrease in fluorescence due to quenching caused by BSA (Marx et al., 2000). P-C6-NBD-PC (0.25 mol %) was incorporated into PC/SM (1:1) LUV before their extrusion as above. Extruded LUVs, at 125 μM lipid, were mixed with 400 μg/ml BSA in elution buffer. The time course of NBD fluorescence emission intensity was measured with the Spex Fluoromax instrument (λ_{ex} 470 nm, slit 1 nm, λ_{em} 530 nm, slit 1 nm) with an integration time of 1 s per point.

RESULTS

Inhibition of sticholysin hemolytic activity by vesicle of different composition

Previous results of our and other laboratories have shown that pre-incubation of actinoporins with lipid SUV inhibits their hemolytic activity. SM was the most effective lipid in this respect. However, associations of this lipid with other components have not been thoroughly studied. We have now compared the remaining hemolytic activity of St I after pre-incubation with SUV of SM, or PC/SM (1:1), or SM/PA (1:1), or only PC (Fig. 1). SM/PA (1:1) vesicles caused the largest inhibition of St I hemolysis, followed by SM, and PC/SM, whereas PC vesicles practically did not cause any inhibition.

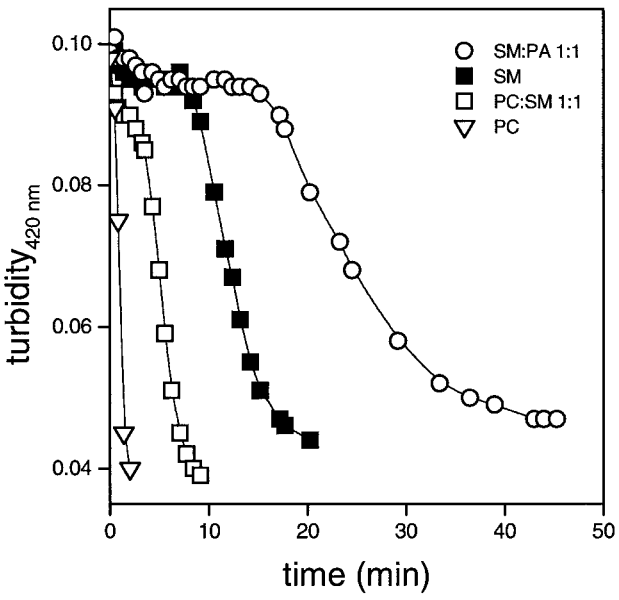

FIGURE 1 Inhibition of St I hemolytic activity by pre-incubation with vesicles of different composition. The time course of hemolysis was followed via the decrease in turbidity of a human red blood cell suspension initially adjusted to an apparent absorbance of 0.1 OD at λ = 420 nm. The toxin was applied either directly or after 30 min of pre-incubation with SUV composed of PC, PC/SM (1:1), SM, SM/PA (1:1) (as indicated), at a lipid/protein molar ratio of 833. The curve with PC SUV was virtually identical to the control with the same dose of cytolysin, but not pre-incubated with the lipid (not shown). Toxin concentration was always 6 nM.

Clearly, vesicles that do not contain SM are poor targets for St I, as it was earlier demonstrated for this (Tejuca et al., 1996) and for other actinoporins (Bernheimer and Avigad, 1976; Macek et al., 1994). However, the inclusion with SM of 50% PA promoted a higher inhibition than inclusion of the same proportion of PC, suggesting a stronger interaction of the protein with vesicles containing a high proportion of this negatively charged phospholipid. We decided to study this effect further, using a direct assay of vesicle permeabilization.

Effect of vesicle composition on the permeabilizing activity of St I and St II

Addition of St I to a solution containing calcein-loaded LUV promoted the release of the dye to a different rate and extent depending on the lipid composition (Fig. 2 *A*). St I and St II are differentiated by 13 amino acid substitutions, scattered throughout the primary sequence, which could in principle originate a different mechanism of action (see, for example, some differences reported for the action of St I and St II in Tejuca et al., 1996 and De Los Rios et al., 1998, respectively, and the different specific hemolytic activity

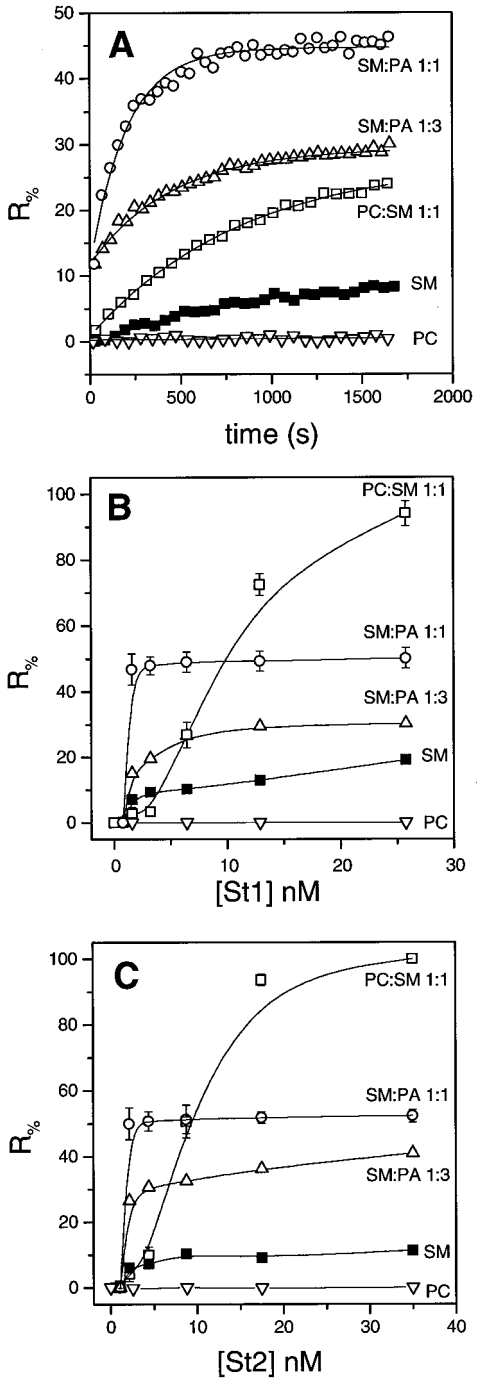

FIGURE 2 Permeabilizing effects of St I and St II on vesicles of different composition. (*A*) Kinetics of release at a small constant dose of St I (6.4 nM) with different lipid compositions. Solid lines are single-exponential relaxations. Vesicles were composed of PC, SM, and PA either as single components or as binary combinations, as indicated (here and in the other panels, the curve with PA alone was superimposed on that of PC alone and was omitted for clarity). Lipid concentration was always ~2 μM. Buffer solution was 100 mM NaCl, 1 mM EDTA, and 10 mM Tris-HCl, pH 7.4. (*B* and *C*) Dose-dependence of the maximal release induced by St I (*B*) or St II (*C*) derived from the steady state of kinetic traces like those in *A*. Points are average ± SEM of 10 determinations for PC/SM (1:1), of two determinations for SM/PA (1:1) and PC, and single values for the others. Solid lines have no theoretical meaning.

(Lanio et al., 2001)). Therefore, we thought that comparing the effects of these two toxins could be important, and in most of the rest will report data obtained with both molecules. Dose-dependence curves of maximal release with LUV of different compositions are shown in Fig. 2, *B* and *C*, for St I and St II, respectively. For vesicles that do not contain SM little or no release was observed, even at high protein concentrations. Vesicles containing SM instead showed a substantial release depending on both the type and the proportion of the other lipid in the mixture. When the various lipid compositions are compared at a low toxin dose, it becomes apparent that SM/PA were more susceptible than SM/PC mixtures, being permeabilized faster and to a higher extent. In addition, lipids mixed in a 1:1 molar ratio showed a higher release than either the single components or most of the nonequimolar mixtures (Fig. 2 and Table 1). Results with St I and St II were similar.

Because the morphological features of vesicles comprising such different components might vary substantially, we characterized them by analyzing their size and fluidity using photon correlation spectroscopy (Fig. 3) and DPH fluorescence polarization, respectively. Indeed, important variations of both parameters were observed. Results are summarized and compared to permeabilization parameters in Table 1. Although the dimensions of vesicles composed of pure PC or PA, or the PC/SM and PC/PS mixtures, were all ~100 nm diameter (as expected from the size of the pores used to extrude them), and the dispersity of the sample was very small (SD ≈ 20 nm), with other compositions this was not always true. The most dramatic deviation was observed for vesicles of pure SM, which appeared to have an average diameter of ~1000 nm and a high polydispersity (SD ≈ 700 nm), suggesting the persistence of a high proportion of multilamellar vesicles.

In view of this, the reduced calcein release observed with SM vesicles may be in part caused by the fact that not all of the inner vesicle compartments are accessible, because St I cannot cross the outer bilayer and reach the internal ones. Nonetheless, this can only be part of the reason, as the observed release was very low, implying that not even the outermost layer was permeabilized. In fact, previous studies on the permeabilization of SM/PC LUV by St I showed a decrease of activity when the amount of SM was increased from 50% to 75% (Tejuca et al., 1996), an effect that was essentially due to a reduced binding.

SM/PA LUV had also larger sizes (between 250 and 330 nm) and a somewhat higher polydispersity (75 nm < SD < 160 nm, see Table 1); therefore, the fact that with these LUVs maximal release saturated ~50% instead of 80%, as with PC/SM, should probably be ascribed to the presence of a certain proportion of oligolamellar structures. Also, in this case release was higher with the mixtures than with the single components. The same is true also for PC/PA vesicles, which had a similar distribution of sizes, and for which

TABLE 1 Physical characteristics of LUV of different compositions and their permeabilization by sticholysins

Lipid Composition*	Diameter† (nm)	SD/Mean‡ (%)	Polarization§	Permeabilization¶ St I R_{max} (%)	St I C_{50} (nM)	St II R_{max} (%)	St II C_{50} (nM)
PC	69	28	0.25	0	—	0	—
PC/SM 1:1	94	22	0.36	96 ± 5	9.7 ± 1	98 ± 2	8.7 ± 1.4
SM	978	71	0.27	19 ± 1	1.6 ± 0.2	14.5 ± 1	1.7 ± 0.2
SM/PA 3:1	324	53	0.20	52 ± 4	1 ± 0.3	51 ± 4	1.8 ± 0.2
SM/PA 1:1	245	34	0.28	50 ± 4	0.8 ± 0.1	51 ± 4	1.6 ± 0.2
SM/PA 1:3	329	47	0.26	30 ± 4	1.6 ± 0.2	41 ± 3	1.9 ± 0.2
PA	168	33	0.22	0	—	0	—
PC/PA 3:1	394	56	0.26	0	—	0	—
PC/PA 1:1	227	52	0.28	7 ± 2	10.9 ± 0.2	13 ± 2	9.7 ± 0.6
PC/PA 1:3	206	40	0.29	0	—	0	—
PC/PS 1:1	96	25	0.22	5 ± 2	8.5 ± 0.2	3 ± 1	16.2 ± 0.9

*LUV composition with indication of molar ratio of mixtures.
†Average size determined by photon correlation spectroscopy.
‡Width of the distribution of vesicle size, i.e., the SD (as obtained from the polydispersity of the cumulant fit (Santos and Castanho, 1996)) expressed as a percent of the mean value.
§Polarization (P) of DPH (Lakowicz, 1983). High polarization values imply higher viscosity, and vice versa, assuming that the fluorescence lifetime is constant.
¶LUV permeabilization, as obtained in Fig. 2. R_{max} is the maximal percentage of release at high toxin doses, whereas C_{50} is the toxin concentration necessary to achieve 50% of R_{max}.

a small but detectable release was observed only for the equimolar mixture. Results with St I and St II were qualitatively similar, as shown by the evaluated parameters reported in Table 1.

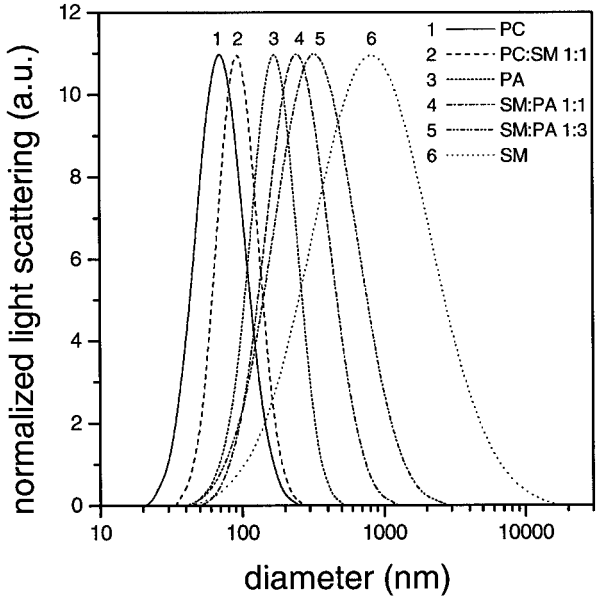

FIGURE 3 Determination of average size and distribution of LUV of different composition by photon correlation spectroscopy obtained as described in the Methods section. Results for the LUV compositions used in Fig. 2 are shown. Values for all compositions used in this paper were measured in the same way and are reported in Tables 1–3.

The role of PA in St I and St II permeabilizing activity

Because PA, and other negatively charged lipids, are mainly concentrated in the inner leaflet of cell membranes and are present only in very small proportions in the outer layer (Connor et al., 1989; Gascard et al., 1991; Langner and Kubica, 1999; Op den Kamp, 1979), we decided to investigate whether PA could have a relevant role in toxin action even at lower, more physiological, concentrations. For this reason we took vesicles composed of PC/SM in a 1:1 molar ratio, as it occurs in many mammalian cells, and added increasing amounts of PA (up to 10 mol %). As reported in Table 2, all these vesicles had homogeneous size (diameter ranging from 110 to 130 nm), and quite narrow polydispersity (15 nm $<$ SD $<$ 24 nm). Interestingly, addition of PA to such PC/SM vesicles elicited a detectable effect on sticholysin activity already at a dose of 0.2 mol %, (Fig. 4 and Table 2). Differences were most evident in C_{50} (i.e., the toxin concentration needed to reach 50% of maximal effect) and in the permeabilization rate. The time course of calcein release induced by St I (and also St II) was reasonably described by a single time constant, τ (Fig. 4 *A*). From this we obtained a permeabilization rate, $k = 1/\tau$, whose dependence on cytolysin concentration and vesicles composition is shown in Fig. 4 *C*. The exponent of the dose dependence and the association constant were derived for both St I and St II (see Appendix) and included in Table 2. The boosting effect of PA was proportional to its amount, becoming maximal at 5 mol %. Because such small proportions are

TABLE 2 Physical characteristics and permeabilization parameters of SM/PC LUV containing different amounts of PA

				Permeabilization							
				St I				St II			
PA* (%)	Diameter† (nm)	SD (%)	P	R_{max} (%)	C_{50} nM	K_{as}‡ (s^{-1} M^{-1})	n§	R_{max} (%)	C_{50} nM	K_{as} (s^{-1} M^{-1})	n
0	94	22	0.36	95 ± 5	9.7	1.8 ± 0.4	1.1	98 ± 2	8.7	0.8 ± 0.4	1.5
0.2	110	17	0.38	86 ± 4	7.0	2.6 ± 0.4	1.1	89 ± 3	7.3	0.8 ± 0.1	1.4
0.5	115	24	0.40	80 ± 3	5.6	4.4 ± 0.6	1.0	84 ± 5	7.1	1.2 ± 0.6	1.4
1	113	18	0.32	81 ± 3	5.0	6.9 ± 0.5	0.8	83 ± 3	6.0	3.2 ± 0.7	1.7
5	112	20	0.35	78 ± 2	2.2	18.6 ± 4.2	1.1	77 ± 3	1.9	18.1 ± 4.1	2.1
10	131	17	0.38	80 ± 2	2.4	13.7 ± 5.0	1.0	80 ± 2	3.3	10.5 ± 3.5	1.8
1 + SA¶ 1%	114	15	0.28	85 ± 1	5.0	5.2 ± 0.1	0.7	91.1 ± 0.1	5.9	2.4 ± 1.0	1.0
1 + SA¶ 2%	119	21	0.32	92 ± 4	4.0	8.3 ± 0.3	0.8	90.6 ± 0.5	4.4	2.3 ± 0.5	1.3

*Molar amount of PA included in the composition.

†Average size, width of the distribution, polarization (P), R_{max}, and C_{50} were all calculated as in Table 1. SD of C_{50} was typically within 5–7% of the mean value.

‡K_{as} is the association rate constant of vesicle permeabilization, calculated for 6.4 nM St I or 8.8 nM St II, assuming $n = 1$. Experiments were done in quadruplicate.

§n is the power dependence of $1/\tau$ on toxin dose (see Fig. 4 *C*).

¶In this case 1% of PA and the reported amount of SA were present.

biologically significant, the role of negative lipids was investigated further.

Effects of different lipids on St I and St II permeabilizing activity

To investigate whether the role of PA in the mechanism of calcein release by actinoporins was peculiar or not, and which were its basis, we compared it to other lipids (Fig. 5 and Table 3). These were all added at a concentration of 5 mol % to PC/SM (1:1) LUV, i.e., the concentration at which PA had optimal effect. Because PA is negatively charged, we first used a series of other acidic lipids that appear in the composition of natural membranes: PG, PI, PS, and CL. Interestingly, all negatively charged lipids had a strengthening effect, but only CL was as efficient as PA. PI, PS, and PG had lower, albeit similar, effects. This was true both in terms of C_{50} (Fig. 5 *B*) and of permeabilization rate (Fig. 5, *A* and *C*), and to a similar extent for either St I or St II (see Table 3). All these vesicles were very homogeneous in size, with a diameter ~110 nm and SD ≈ 20 nm (Table 3).

A possible explanation for the effects of negatively charged lipids was that the negative surface potential they create could attract the basic toxins. To control this, similar experiments were performed including the zwitterionic phospholipid PE or the positively charged lipid SA. Surprisingly, these two lipids also produced a certain extent of enhancement of St I and St II permeabilization (Fig. 5 and Table 3). Maximal release in the presence of SA was lower; however, although the size and dispersity of PE-containing vesicles was normal, that of SA-containing LUV was larger, 240-nm diameter, and polydisperse, SD ≈ 100 nm (Table 3). In view of this, because PC/SM/SA LUV probably contain also oligolamellar vesicles that do not permit a complete calcein release, the enhancement observed with SA was probably almost as significant as that with PE and PS. Therefore, a role of a negative surface potential does not seem to be purported.

This was further investigated using mixtures in which both PA and SA were present. The stimulating effect of 1% of negatively charged PA was not decreased by the simultaneous presence of even twice as much positively charged SA, confirming that the generation of a negative surface potential was not the boosting mechanism (Fig. 6 and Table 2).

Effects of ionic strength on the permeabilization of vesicles with and without PA

To further assess whether an electrostatic interaction mediated by surface charges was involved in actinoporin permeabilization, we studied the effects of ionic strength. It is known, in fact, that increasing the ionic strength decreases the electrostatic interactions via charge screening. To avoid any possible influence of changes in vesicle shape due to transmembrane salt gradients, in these experiments we kept constant the total osmolarity of the solution by adding suitable amounts of sucrose. Indeed, we observed that sticholysin-induced calcein release from PC/SM/PA LUV (5 mol % PA) was influenced by the ionic strength (Fig. 7 *A*). At all toxin doses, a certain decline of activity was observed in increasing salt concentration above 200 mM. However, these effects were not due to an electrostatic interaction between the negative charge of PA and the positive charge of the protein because uncharged vesicles, comprising only zwitterionic lipids (PC and SM), displayed an even greater decrease (Fig. 7 *B*). The results with St II are shown in Fig. 7; however, the same was observed also with St I. There-

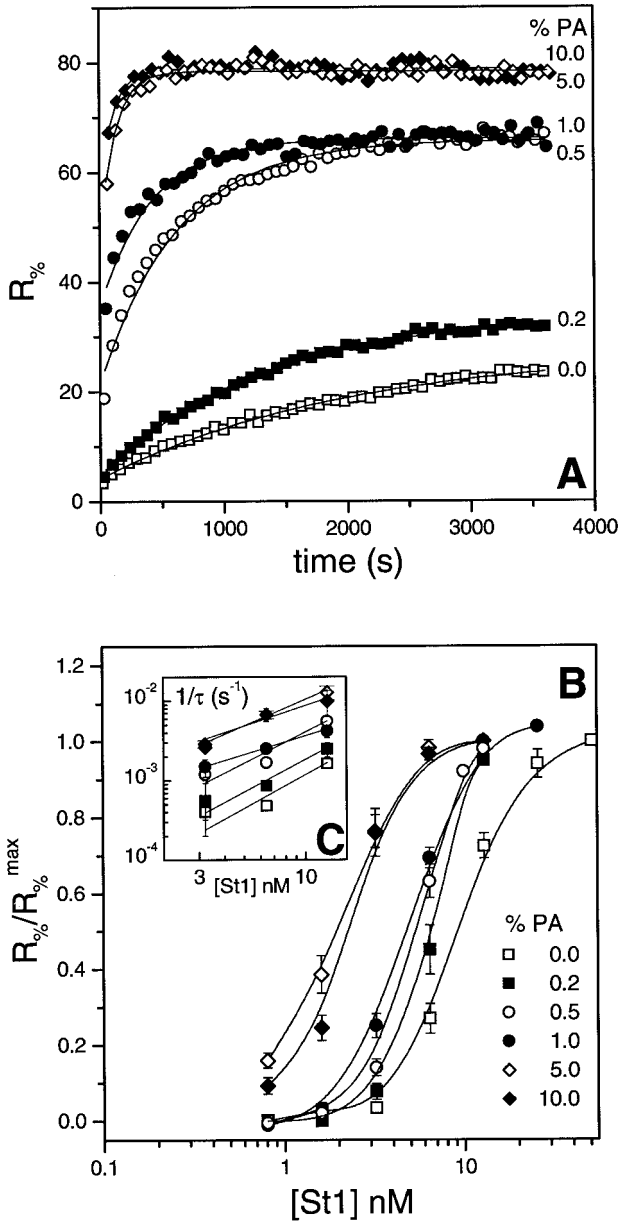

FIGURE 4 Effects of increasing PA content in PC/SM (1:1) LUVs on the permeabilization by St I. (*A*) Kinetics of release at a constant dose of St I (6.4 nM) with different percentage amounts of PA (as indicated). Lipid concentration was always ~2 μM, other conditions as in Fig. 2. The kinetic were fitted to a single-exponential relaxation with time constant τ. (*B*) Dose-dependence of calcein release induced by St I derived from the steady state of kinetics like those in *A*. The maximal release obtained at high toxin doses (R_{max}) was slightly different with the different lipid compositions (most probably because of changes in the small proportion of oligolamellar vesicles remaining in the preparation). Therefore, the reported release values (R%) have been normalized by dividing by R_{max}. The values of R_{max} used are reported in Table 2. Points are average ± SEM of four determinations (except for control, which are average ± SEM of 10 determinations). Solid lines have no theoretical meaning. (*C*) Double-logarithmic concentration-dependence of the permeabilization rate $1/\tau$. The time constant τ was obtained by the single-exponential fit of kinetic traces like those shown in *A*. A linear regression provided the exponent of the dose-dependence reported in Table 2.

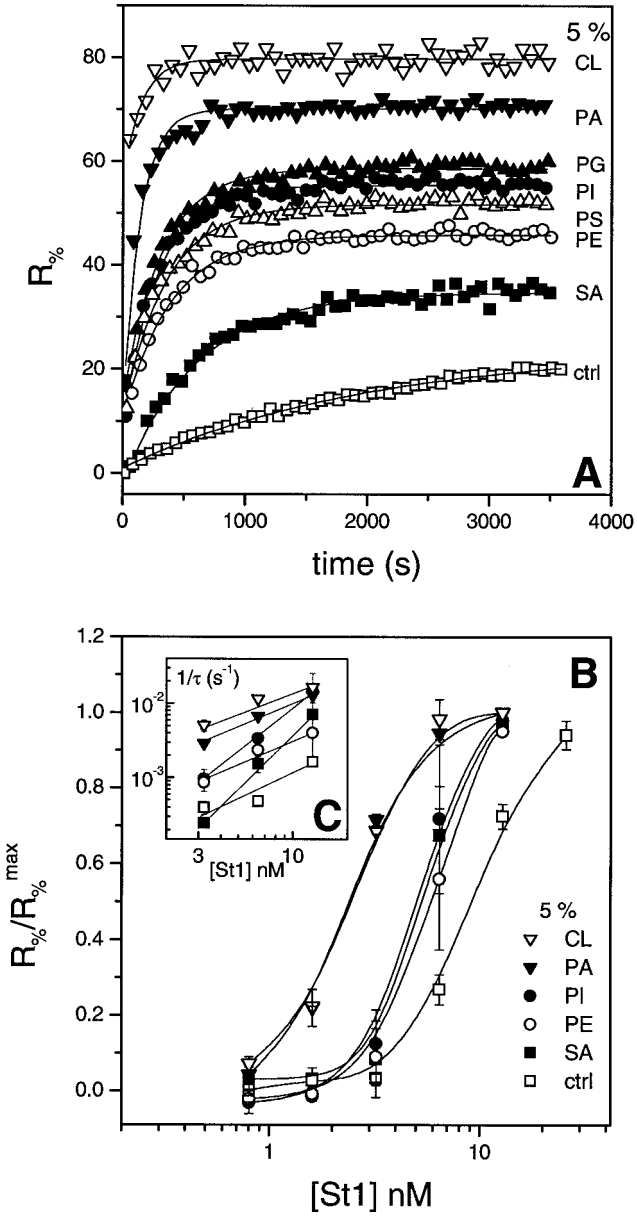

FIGURE 5 Effects of including 5 mol % of different lipids into PC/SM (1:1) LUVs on their permeabilization by St I. (*A*) Kinetics of release at a constant dose of St I (6.4 nM) with different compositions. The kind of lipid present at 5% in the LUV composition is indicated. With CL, which has double charge and double mass compared to other acidic phospholipids, the included molar amount was 2.5% and the molar ratio of negative charges was 5%. Lipid concentration was always ~2 μM, other conditions as in Fig. 2. The kinetics were fitted to a single-exponential relaxation with time constant τ. Here and in the other panels, curves with 5% PS and PG were practically superimposed on that with 5% PI and were omitted for clarity. (*B*) Dose-dependence of calcein release induced by St I derived from the steady state of kinetics as in *A*. Also in this case the reported release was normalized by dividing by R_{max}. The values of R_{max} used are given in Table 3. Points are average ± SEM of four determinations (or average ± SEM of 10 determinations for control). Solid lines have no theoretical meaning. (*C*) Concentration-dependence of the permeabilization rate $1/\tau$, where τ was obtained by the single-exponential fit of kinetic traces like those in *A*. Linear regression of the double-logarithmic dose-dependence provided the exponent n reported in Table 3.

TABLE 3 Physical characteristics and permeabilization parameters of SM/PC (1:1) LUV containing 5% of different lipids

				Permeabilization							
				St I				St II			
Added Lipid	Diameter* (nm)	SD (%)	P	R_{max} (%)	C_{50} nM	K_{as}	n	R_{max} (%)	C_{50} nM	K_{as}	n
—	94	22	0.36	95 ± 5	9.7	1.7 ± 0.4	1.1	98 ± 2	8.7	0.8 ± 0.4	1.4
PA	112	20	0.35	78 ± 2	2.3	18.6 ± 4.2	1.0	77 ± 2	3.9	18.1 ± 4.1	2.1
CL	106	23	0.16	81 ± 2	2.6	36.0 ± 7.1	0.9	87 ± 1	3.3	32.7 ± 0.1	1.0
PG	108	21	0.20	82 ± 2	5.3	9.4 ± 2.9	1.5	83 ± 1	7.2	2.6 ± 0.5	2.0
PI	117	18	0.32	80 ± 2	5.2	8.6 ± 2.4	2.0	80 ± 1	7.8	1.7 ± 0.1	3.2
PS	116	20	0.32	79 ± 2	5.5	7.2 ± 3.0	1.8	78 ± 2	7.8	1.0 ± 0.6	1.5
PE	113	21	0.39	82 ± 2	6.0	6.5 ± 3.4	0.8	82 ± 2	7.5	1.3 ± 0.1	2.8
SA	239	43	0.34	54 ± 2	5.5	0.9† ± 0.3	1.9	54 ± 4	7.6	0.4† ± 0.1	1.6

*Average size, width of the distribution, polarization (P), R_{max}, C_{50}, K_{as}, and n were all calculated as in Tables 1 and 2. Experiments were done in quadruplicate.

†This small value of the normalized association constant K_{as} originates from the larger size of the vesicles (see Eq. A5).

fore, the peculiar effects of PA (and CL) do not seem to depend on their charge.

Effects of St I on the rate of lipid flip-flop in the vesicles

We decided to further investigate the nature of the interaction of St I with lipids by determining the transmembrane movement of a fluorescent lipid included in the bilayer, by the method of extraction of short chain lipids by BSA (Marx et al., 2000). It was described, in fact, that some cytolysins may increase the rate of transbilayer movement of lipid molecules (Classen et al., 1987; Schneider et al., 1986). That this is the case also for sticholysins is indicated by the experiment reported in Fig. 8. The amount of labeled lipid extracted by BSA in the external compartment was doubled by the subsequent addition of St I. Instead, if St I was present from the beginning, the amount available for BSA extraction was already double that in the absence of St I, even if St I itself did not effect any extraction. Because the spontaneous flip-flop of lipids is a very slow event in the absence of a specific enzymic flippase ($t_{1/2}$ of days, see Schneider et al., 1986), BSA is expected to extract only the lipids in the outer layer. However, the addition of the sticholysin also clearly promoted the accessibility of BSA to the inner layer. Because BSA cannot permeate through the St I pore and LUV are not broken by sticholysins at this lipid-to-toxin ratio (Tejuca et al., 1996), this implies that St I promotes the transfer of lipids from the inner to the outer layer, similarly to other pore-forming peptides (Classen et al., 1987; Schneider et al., 1986). The effect depends on the dose of St I (Fig. 8, *inset*) and saturates at a total amount of mobilized lipid that is ~70% of that apparently made accessible by Tx100. This is probably a lower limit, because Tx100 may affect the fluorescence of the label either directly or indirectly by diminishing the light scattering. In addition, the incomplete mobilization observed may reflect, at least in part, the presence of some oligolamellar structures, because in that case neither St I nor BSA can cross the outer bilayer and all the label on the internal layers would remain unextracted.

DISCUSSION

Inhibition of hemolytic activity (Fig. 1) and a direct permeabilization assay (Fig. 2) both indicate that sticholysins interact preferentially with SM-containing membranes, as it was consistently observed by all researchers in the field (Kem, 1988; Macek, 1997; Macek et al., 1994; Turk, 1991). The fact that pure SM membranes are better than PC/SM membranes for inhibition of hemolysis, but not for permeabilization, is not a contradiction because the first experiment was performed with SUV and the latter with LUV. We have already shown that SUV of pure SM are better permeabilized than LUV of the same composition, and this was attributed to the high packing of the headgroups in LUV, which is not present in SUV (Tejuca et al., 1996). It was supposed that a steric barrier did not allow adequate interaction of the protein with the SM headgroup, a preliminary step for its binding and proper insertion into the bilayer. It appears, in fact, that actinoporins recognize SM both at the level of the headgroup, as indicated by the fact that SM analogs with a modified phosphoric group are resistant to these toxins (Meinardi et al., 1995), and by the ceramide moiety, because the ganglioside GM_1, with the same ceramide moiety as SM, could mimic its action (Macek et al., 1994).

When different binary combinations of PC, SM, and PA were compared for permeabilization by sticholysins, two facts were clear: mixtures in general are more sensitive that single lipids, and the presence of PA was a strong promoter of toxin action. The fact that PA-containing vesicles were more susceptible to sticholysins was analyzed in further detail by incorporating small amounts of this lipid into

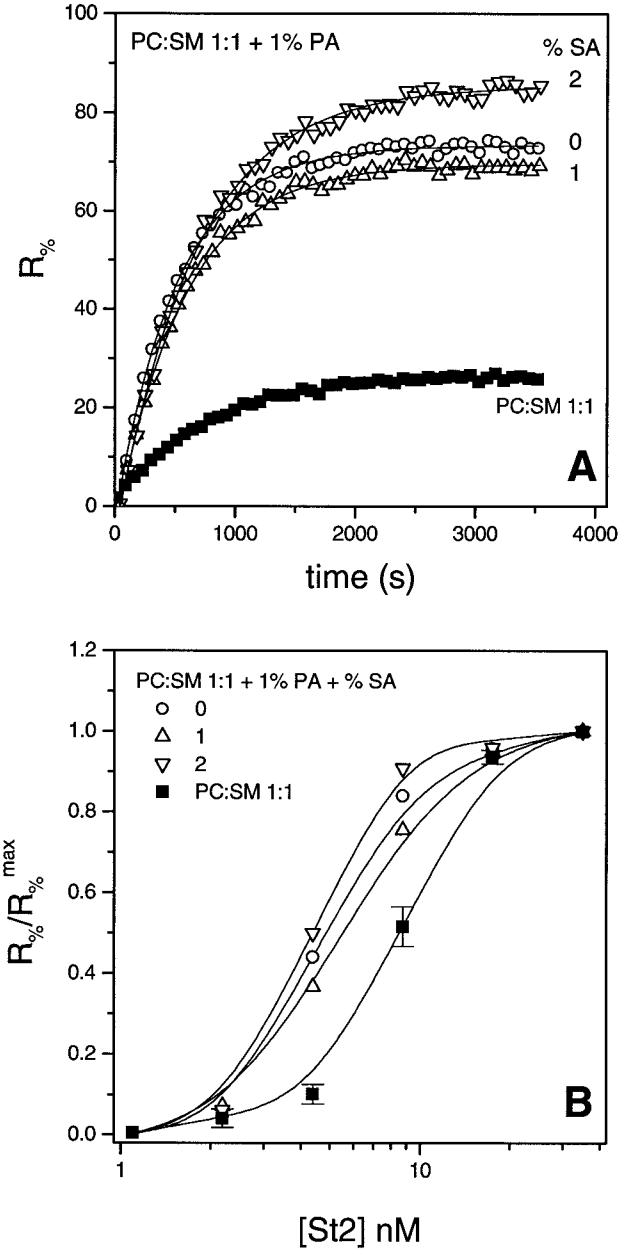

FIGURE 6 Effects of co-including negatively and positively charged lipids into PC/SM (1:1) LUVs on their permeabilization by St II. (*A*) Kinetics of release at a constant dose of St II (8.8 nM) with different compositions. Filled symbols are for control vesicles containing only PC and SM in a 1:1 molar ratio. Empty symbols are for LUVs with the addition of 1% negatively charged PA and 0, 1, or 2% positively charged SA (as indicated). Lipid concentration was always ~2 μM, other conditions as in Fig. 2. The kinetics were fitted to a single-exponential relaxation with time constant τ. (*B*) Dose-dependence of calcein release induced by St II derived from the steady state of kinetics as in *A*. Also in this case the reported release was normalized by dividing by R_{max}. The values of R_{max} used are given in Table 2. The outcome of one of two sets of experiments, giving consistent results, is reported. Points of control are average ± SEM of 10 determinations. Solid lines have no theoretical meaning. The linear regression of the double logarithmic dose-dependence of $1/\tau$ was performed also in this case and the derived exponent was included in Table 2.

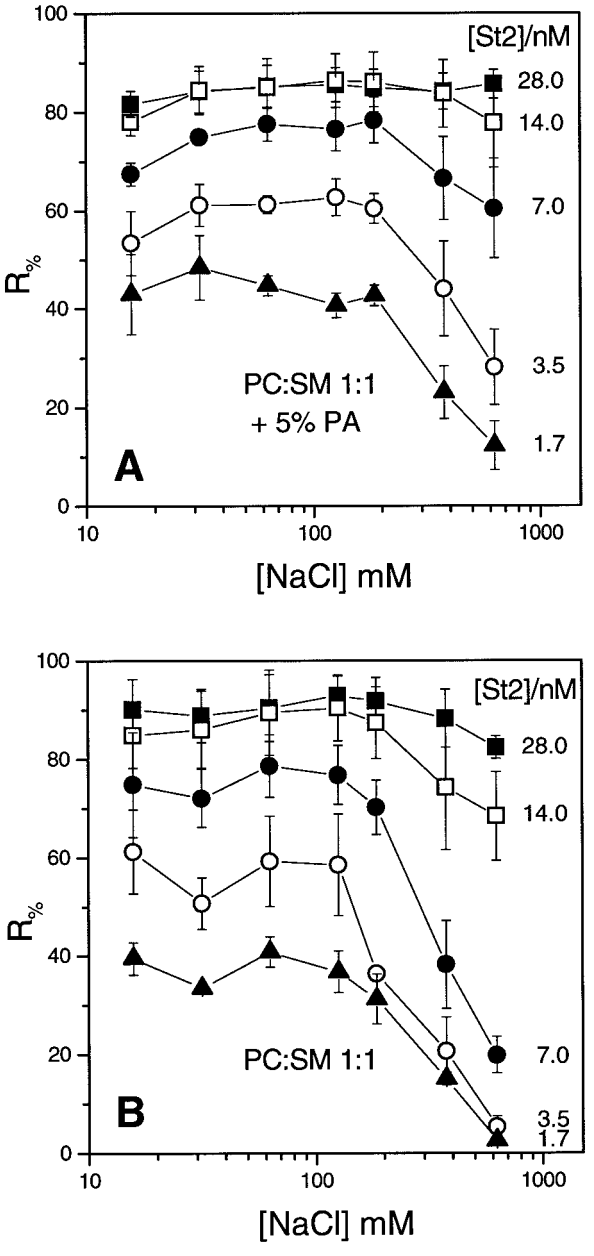

FIGURE 7 Effect of ionic strength on St II permeabilization of PC/SM (1:1) LUVs with or without 5 mol % PA. The buffer contained 1 mM EDTA, 10 mM Tris-HCl buffering at pH 7.4, and the indicated concentration of NaCl, while the total osmolarity was kept constant at 1277 mM by the addition of sucrose. Lipid concentration was 2 μM, whereas the toxin dose was varied as indicated. Results for LUVs that did or did not contain the negatively charged lipid are reported in *A* and *B*, respectively. Points are average ± SEM of four determinations in *A* and two in *B*. Results with St I were completely consistent (not shown).

susceptible vesicles composed of PC/SM (1:1). We observed significant effects starting at very low PA concentrations, below 5%. One possible hypothesis was that the negative surface potential generated by PA attracts the basic cytolysins thus improving their membrane insertion. How-

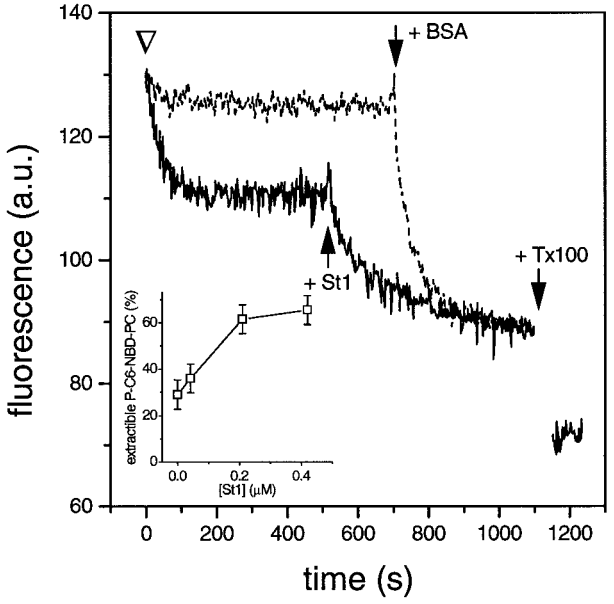

FIGURE 8 Effects of St I on the rate of transmembrane movement of a fluorescent lipid. PC/SM (1:1) LUVs were prepared with the inclusion of 0.25% of a short-chain fluorescent lipid (P-C6-NBD-PC), and the NBD fluorescence was measured at λ_{ex} 470 nm, λ_{em} 530 nm (lipid 125 μM). At the time indicated by the empty arrowhead either St I (*upper dashed trace*) or BSA (*lower continuous trace*) was added in the external compartment at a concentration of 0.42 and 5.8 μM, respectively. BSA, but not St I (*lower versus upper trace*), caused a substantial decrease of the fluorescence due to the quenching of the extracted lipid (Marx et al., 2000). Subsequent addition of St I (0.42 μM) to toxin-free vesicles (*arrow, lower trace*), induced a further decrease of the fluorescence of an amount equivalent to the initial decay. Conversely, addition of BSA (5.8 μM) to St I pre-treated LUVs (*arrow, upper trace*), caused an immediate decrease of fluorescence equivalent to the sum of the two steps observed when the reagents were added in the opposite order. NBD fluorescence with completely solubilized LUVs was determined adding 1 mM Tx100 (*arrow*). One of three equivalent experiments is shown. *Inset:* Decrease of fluorescence induced by BSA, at steady state, in the presence of different doses of St I. Values are expressed as a percentage of the decrease observed in the presence of Tx100. Other experimental conditions: buffer solution, 100 mM NaCl, 1 mM EDTA, and 10 mM Tris-HCl, pH 7.4

ever, our results demonstrate that the surface potential generated by negatively charged lipid is not a determining factor for pore formation by St I and St II. In fact, 1) other lipids, even neutral or positively charged, induced enhancing effects; 2) there was no inhibitory effect of increased ionic strength that could be ascribed to screening of the surface potential; and 3) co-inclusion with PA of even twice as much positively charged SA did not decrease the boosting effect. With regard to the second point, i.e., the inhibitory effect of high ionic strength with or without PA, it could either be related to a protein conformational change induced by high ionic strength, rendering the cytolysin less competent to permeabilize the LUV, or to a strengthening of the hydrophobic forces within the protein, preventing a conformational change necessary for lipid binding, which conceivably implies the exposure of a normally hidden hydrophobic patch.

When different lipids were compared, all as 5% molar inclusions in PC/SM LUV, it was observed that most of them had strengthening effects on sticholysin action, i.e., reduction of C_{50} and increase of association constant; however, PA and CL elicited the strongest effects (Fig. 5 and Table 3). This action is poorly related to the effects of these lipid components on membrane viscosity, as indicated by comparison with the measured DPH polarization (Tables 1–3). For example, PA didn't change LUV viscosity, whereas CL strongly decreased it, but both had the same strong boosting effect on pore formation; similarly, PE increased LUV viscosity, whereas PG markedly decreased it, yet they elicited a very similar stimulation of sticholysin action, lower than that of PA and CL (Table 3). Interestingly, among the lipids tried, PA and CL are the strongest inducers of negative curvature in the bilayer (Cullis and de Kruijff, 1979; Farren et al., 1983; Seddon, 1990; Seddon et al., 1983), and this property might be relevant. In fact, it was recently suggested that the opening of some toxin channel might be accompanied by the formation of a toroidal lipid pore surrounding the toxin structure (Epand, 1998). In such a toroidal arrangement, exemplified in Fig. 9, a positive curvature is observed perpendicular to the plane of the membrane, but a negative curvature is present in the plane of the membrane all around the pore. Therefore, it is possible that the presence of minor amounts of lipids that favor

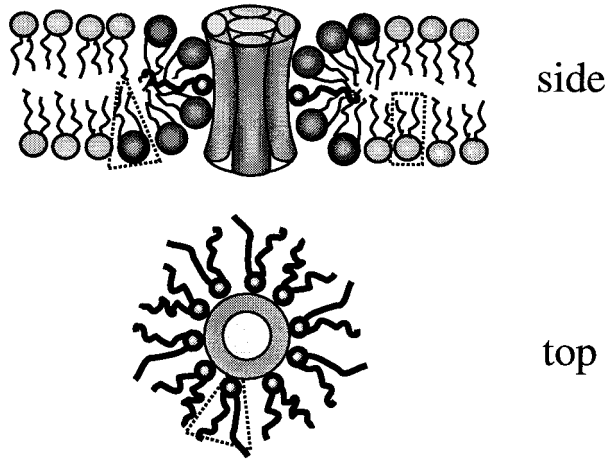

FIGURE 9 Cartoon of the lipid organization around the transmembrane part of the pore formed by sticholysins. This is represented as a cylinder of ~5 nm length (the thickness of the membrane) and 2 nm diameter (Tejuca et al., 1996) built around 4–5 α-helices. Around the toxin channel a toroidal lipid pore is formed. Lipids inducing positive curvature (conical shape with headgroup at the base) are favored in the section of the lipid torus perpendicular to the plane of the membrane (*side view*); lipids inducing negative curvature (conical shape with headgroup at the tip, like PA and CL) are favored in the central section parallel to the plane of the membrane (*top view*). Lipids with cylindrical shape (e.g., PC and SM) are preferred in the lamellar phase.

this nonlamellar organization could also augment the efficiency of toxin pore formation. Interestingly, it has been found that in lipid membranes containing mixed cationic and anionic lipids the order of propensity for the nonlamellar phase is PA > CL > PG > PS (Lewis and McElhaney, 2000). This is practically the same order that we have observed for the stimulation of pore formation (Fig. 5). In our case, the positive charge, essential to compensate for the electrostatic repulsion between negatively charged headgroups, might be provided by basic residues present on the transmembrane section of the toxin. Besides inducers of negative curvature, such as the negatively charged lipids above and PE (Cullis and de Kruijff, 1979; Seddon, 1990), SA also has a strengthening effect (Fig. 5). SA, as a single chain lipid, is normally an inducer of positive curvature (Cullis and de Kruijff, 1979; Seddon, 1990) and as such could help in stabilizing the profile of the toroidal pore perpendicular to the membrane.

A similar toroidal pore has been proposed for the action of the cationic antimicrobial peptide magainin (Matsuzaki, 1998, 1999) and experimental evidence has recently been found (Yang et al., 2000). The magainin pore is lined by seven copies of the molecule arranged in an α-helical structure and has a diameter of ~3.5 nm. The diameter of the pore formed by sticholysins is ~2.2 nm (De Los Rios et al., 1998; Tejuca et al., 1996), and thus could involve only four or five similar structures, in agreement with the fact that the average stoichiometry of actinoporin channels is believed to be a tetramer (Belmonte et al., 1993; De Los Rios et al., 1999; Varanda and Finkelstein, 1980). A putative region of the actinoporin that could be involved in crossing the membrane is an amphipathic α-helix located at the N-terminus which was predicted, on the basis of the primary structures, to be a conserved element of all actinoporins (Anderluh et al., 1999b; Belmonte et al., 1994; Macek et al., 1994). This helix has striking homology with bee venom melittin and other cytolytic basic peptides of this family, which all adopt α-helical structure (Belmonte et al., 1994). It carries, at the C-terminal side, a cluster of three positively charged residues (K^+-S-V-R^+-K^+) that could interact with acidic lipids. The interaction of this N-terminal region with the lipid membrane was demonstrated for equinatoxin II (Eqt II), one of the best-studied actinoporins, by introducing single cysteins in this region which were then labeled with the lipid-sensitive probe acrylodan (Anderluh et al., 1999a). Furthermore, the existence of an α-helix at the N-terminus of Eqt II has been now unequivocally established by crystallographic x-ray analysis (Gregor Anderluh, personal communication). In the same cystein scanning work (Anderluh et al., 1999a), it was demonstrated that at least one other portion of the molecule interacts with the lipid (i.e., a cluster of tryptophan residues located around position 115), and this can provide the basis for the higher affinity of actinoporins to model and cell membranes as compared to most small α-helical cytotoxic peptides (Cornut et al., 1993). Finally, it is worth mentioning that the diameter of the lipid-surrounded aqueous pore that is observed in the inverse hexagonal lipid phase (H_{II}), whose arrangement is similar to the central part of the toroidal pore of Fig. 9, is ~3–5 nm, depending on the lipid present (Seddon, 1990), i.e., exactly in the range necessary for surrounding the sticholysin pore.

One implication of the toroidal model is that each pore behaves as a point of fusion of the inner lipid monolayer with the outer one. This structure would clearly favor the transbilayer movement of lipid molecules, which is otherwise severely restricted in purely lipidic membranes. Indeed, we have observed that St I induces mobilization of inner layer lipids in a dose-dependent way (Fig. 8), thus providing further evidence for the toroidal pore model. A similar induction of transmembrane movement of lipid has been observed also with other cytolytic peptides such as gramicidin (Classen et al., 1987) and amphotericin B, but also with a bacterial cytotoxin (Schneider et al., 1986). It is possible that a similar mechanism of formation of nonlamellar phases was involved. In this regard it is worth remembering that at least two other peptides have been reported to promote the formation of a nonlamellar phase in membranes, e.g., gramicidin S (Staudegger et al., 2000) and alamethicin (Ionov et al., 2000). A model with some similarities, called the "carpet model," has been proposed as a general mechanism of action of amphipathic α-helical antimicrobial peptides (Oren and Shai, 1998). Such a model also implies the formation of nonlamellar lipid structure; however, in that case, the structure is much less ordered and involves the presence of a high number of peptides. Our model is also different from those used for large-molecular-weight bacterial pore-forming toxins, which are essentially of two types (Lacy and Stevens, 1998; Lesieur et al., 1997): the β-barrel model (whose prototype is the channel formed by *Staphylococcus aureus* α-toxin), and the α-helical bundle model (introduced for colicins and *Bacillus thuringiensis* δ-endotoxins). It is also different from the β-barrel model presented for *B. thuringiensis* cytocidal toxin (Lesieur et al., 1997; Li et al., 1996), a molecule of size similar to the actinoporins, but it should be mentioned that this model was recently questioned, and the involvement of two toxin α-helices was also invoked in that case (Gazit et al., 1997), which could have some similarity with actinoporins. This apparent uniqueness may reflect the fact that actinoporins are eukaryotic proteins and they are unrelated to any other known protein, thus having the potential for a peculiar mode of action.

APPENDIX

The kinetics of LUV permeabilization by sticholysins was analyzed in terms of a simplified model, based on reaction rate theory, that we have introduced earlier (Menestrina et al., 1989), with only minor modifications.

As already shown, sticholysins form pores in lipid vesicles through which entrapped calcein can flow out (Tejuca et al., 1996). Because of the

small dimensions of these vesicles the formation of just one channel, with the conductance found in Tejuca et al. (1996), will release all the internal calcein in a few milliseconds. Therefore, the rate-limiting event in our experiments is the formation of pores and not the release of the marker. Accordingly, we introduce a phenomenological reaction scheme for the formation of oligomeric sticholysin pores:

$$\underbrace{T_f + T_f + \cdots + T_f}_{n} + L \underset{K_{dis}}{\overset{K_{as}}{\rightleftharpoons}} P \qquad (A1)$$

where T_f and P represent free toxin and pores, respectively, and K_{as}, K_{dis} the rate constants for association and dissociation. We will consider here that the aggregation mechanism necessary to form the pore is sufficiently represented by the experimentally determined exponent n, which does not necessarily reflect the real number of monomers forming the pore. It follows from scheme A1 that:

$$d[P]/dt = K_{as}[T_f]^n[L] - K_{dis}[P] \qquad (A2)$$

where quantities in square brackets are concentrations, and L indicates total lipid available in the form of vesicles

We further assume that K_{dis} is negligibly small, on the basis of the fact that binding to vesicles is virtually irreversible (as indicated by the inhibition experiments in Fig. 1 and previously demonstrated (Tejuca et al., 1996)). We can therefore rewrite Eq. A2 as:

$$d[P]/dt = K_{as}[T_f]^n[L] \qquad (A3)$$

[L] is related to the concentration of vesicles, [V], by

$$[L] = [V]\mu\beta \qquad (A4)$$

where μ is the average number of lipid molecules per vesicle, typically 10^5 in our experiments, and β is the fraction of lipid that is located in the outer leaflet, ~0.5.

In a normal experiment $[T_f]$ is ~8 nM, while the total concentration of vesicles, V_o, is 0.02 nM. Because permeabilization is well below 100%, it follows that some of the vesicles carry no channels and hence that only very few of them, if any, carry more than one. Therefore, we can reasonably assume that permeabilized vesicles contain only one channel and thus that $[T_f]$ remains practically constant throughout the reaction (first-order approximation). Accordingly, we introduce a new rate constant:

$$K^* = K_{as}[T_f]^n\mu\beta \qquad (A5)$$

If each permeabilized vesicle carries only one channel, we get the following expression for the concentration of intact vesicles [V]:

$$[V] = V_o - P \qquad (A6)$$

Under these conditions Eq. A3 is easily integrated using Eqs. A4–A6 to obtain

$$[V] = V_o \exp(-t/\tau) \qquad (A7)$$

where τ is an apparent time constant for the rate of disappearing of intact vesicles related to K^* by

$$K^* = 1/\tau \qquad (A8)$$

For the total fluorescence F, our observable, we have that

$$F = F_o(V_o - [V]) = F_oV_o(1 - \exp(-t/\tau)) \qquad (A9)$$

where F_o is the contribution to fluorescence of the content released by one mole of vesicles. Fitting Eq. A9 to the time course of sticholysin-induced fluorescence increase, we estimated the time constant τ and from this the association constant:

$$K_{as} = 1/(\tau[T_f]^n\mu\beta) \qquad (A10)$$

which is reported in Tables 2 and 3 together with the exponent n.

We thank Gregor Anderluh for a critical reading of the manuscript.

This work was financially supported by the Italian Consiglio Nazionale delle Ricerche, by a grant from the Istituto Trentino di Cultura (to C.A.V. and I.B.), and by a fellowship from the Comune di Trento (to C.P.).

REFERENCES

Ahnert-Hilger, G., and U. Weller. 1997. Alpha-toxin and streptolysin O as tools in cell biological research. *In* Cell Biology: A Laboratory Handbook. J. E. Celis, editor. Academic Press, New York. 103–110.

Alouf, J. E., and C. Geoffroy. 1991. The family of the antigenically-related, cholesterol-binding ("sulphydryl-activated") cytolytic toxins. *In* Source Book of Bacterial Protein Toxins. J. E. Alouf and J. H. Freer, editors. Academic Press, London. 147–186.

Alvarez, C., M. E. Lanio, M. Tejuca, D. Martinez, I. F. Pazos, A. M. Campos, M. V. Encinas, T. Pertinhez, S. Schreier, and E. Lissi. 1998. The role of ionic strength on the enhancement of the hemolytic activity of sticholysin 1, a cytolysin from *Stichodactyla helianthus*. *Toxicon.* 36:165–178.

Al-yahyaee, S. A. S., and D. J. Ellar. 1996. Cell targeting of a pore-forming toxin, CytA δ-endotoxin, from *Bacillus thuringiensis* subspecies *israelensis*, by conjugating CytA with anti-thy 1 monoclonal antibodies and insulin. *Bioconjugate Chem.* 7:451–460.

Anderluh, G., A. Barlic, Z. Podlesek, P. Macek, J. Pungercar, F. Gubensek, M. Zecchini, M. Dalla Serra, and G. Menestrina. 1999a. Cysteine scanning mutagenesis of an eucaryotic pore-forming toxin from sea anemone: topology in lipid membranes. *Eur. J. Biochem.* 263:128–136.

Anderluh, G., I. Krizaj, B. Strukelj, F. Gubensek, P. Macek, and J. Pungercar. 1999b. Equinatoxins, pore-forming proteins from the sea anemone *Actinia equina*, belong to a multigene family. *Toxicon.* 37: 1391–1401.

Bayley, H. 1995. Pore-forming proteins with built-in triggers and switches. *Bioorg. Chem.* 23:340–354.

Belmonte, G., G. Menestrina, C. Pederzolli, I. Krizaj, F. Gubensek, T. Turk, and P. Macek. 1994. Primary and secondary structure of a pore-forming toxin from the sea anemone, *Actinia equina* L., and its association with lipid vesicles. *Biochim. Biophys. Acta.* 1192:197–204.

Belmonte, G., C. Pederzolli, P. Macek, and G. Menestrina. 1993. Pore formation by the sea anemone cytolysin equinatoxin II in red blood cells and model lipid membranes. *J. Membr. Biol.* 131:11–22.

Bernheimer, A. W. 1990. Cytolytic peptides of sea anemones. *In* Marine Toxins: Origin, Structure and Molecular Pharmacology. S. Hall and G. Strichartz, editors. American Chemical Society, Washington, DC. 304–311.

Bernheimer, A. W., and L. S. Avigad. 1976. Properties of a toxin from the sea anemone *Stoichactis helianthus*, including specific binding to sphingomyelin. *Proc. Natl. Acad. Sci. U.S.A.* 73:467–471.

Bhakdi, S., U. Weller, I. Walev, E. Martin, D. Jonas, and M. Palmer. 1993. A guide to the use of pore-forming toxins for controlled permeabilization of cell membranes. *Med. Microb. Immunol.* 182:167–175.

Classen, J., C. W. M. Haest, H. Tournois, and B. Deuticke. 1987. Gramicidin-induced enhancement of transbilayer reorientation of lipids in the erythrocyte membrane. *Biochemistry.* 26:6604–6612.

Connor, J., C. Bucana, I. J. Fidler, and A. J. Schroit. 1989. Differentiation-dependent expression of phosphatidylserine in mammalian plasma membranes: quantitative assessment of outer-leaflet lipid by prothrombinase complex formation. *Proc. Natl. Acad. Sci. U.S.A.* 86:3184–3188.

Cornut, I., E. Thiaudière, and J. Dufourcq. 1993. The amphipathic helix in cytotoxic peptides. *In* The Amphipathic Helix. R. M. Epand, editor. CRC Press, Boca Raton, FL. 173–219.

Cullis, P. R., and B. de Kruijff. 1979. Lipid polymorphism and the functional roles of lipids in biological membranes. *Biochim. Biophys. Acta.* 559:399–420.

Dalla Serra, M., G. Fagiuoli, P. Nordera, I. Bernhart, C. Della Volpe, D. Di Giorgio, A. Ballio, and G. Menestrina. 1999. The interaction of lipodepsipeptide toxins from *Pseudomonas syringae* pv. *syringae* with biological and model membranes: a comparison of syringotoxin, syringomycin and syringopeptins. *Mol. Plant - Microbe Interact.* 12:391–400.

De Los Rios, V., J. M. Mancheno, M. E. Lanio, M. Onaderra, and J. G. Gavilanes. 1998. Mechanism of the leakage induced on lipid model membranes by the hemolytic protein sticholysin II from the sea anemone *Stichodactyla helianthus*. *Eur. J. Biochem.* 252:284–289.

De Los Rios, V., J. M. Mancheno, A. Martinez del Pozo, C. Alfonso, G. Rivas, M. Onaderra, and J. G. Gavilanes. 1999. Sticholysin II, a cytolysin from the sea anemone *Stichodactyla helianthus*, is a monomer-tetramer associating protein. *FEBS Lett.* 455:27–30.

Edidin, M. 1997. Lipid microdomains in cell surface membranes. *Curr. Opin. Struct. Biol.* 7:528–532.

Epand, R. M. 1998. Lipid polymorphism and protein-lipid interactions. *Biochim. Biophys. Acta.* 1376:353–368.

Farren, S. B., M. J. Hope, and P. R. Cullis. 1983. Polymorphic phase preference of phosphatidic acid: a ^{31}P and ^{2}H NMR study. *Biochem. Biophys. Res. Commun.* 111:675–682.

Fivaz, M., L. Abrami, and F. G. van der Goot. 1999. Landing on lipid rafts. *Trends Cell Biol.* 9:212–213.

Gascard, P., D. Tran, M. Sauvage, J. C. Sulpice, K. Fukami, T. Takenawa, M. Claret, and F. Giraud. 1991. Asymmetric distribution of phosphoinositides and phosphatidic acid in the human erythrocyte membrane. *Biochim. Biophys. Acta.* 1069:27–36.

Gazit, E., N. Burshtein, D. J. Ellar, T. Sawyer, and Y. Shai. 1997. *Bacillus thuringiensis* cytolytic toxin associates specifically with its synthetic helices A and C in the membrane bound state. Implications for the assembly of oligomeric transmembrane pores. *Biochemistry.* 36: 15546–15554.

Gu, L. Q., O. Braha, S. Conlan, S. Cheley, and H. Bayley. 1999. Stochastic sensing of organic analytes by a pore-forming protein containing a molecular adapter. *Nature.* 398:686–690.

Hatakeyama, T., T. Sato, E. Taira, H. Kuwahara, T. Niidome, and H. Aoyagi. 1999. Characterization of the interaction of hemolytic lectin CEL-III from the marine invertebrate, *Cucumaria echinata*, with artificial lipid membranes: involvement of neutral sphingoglycolipids in the pore-forming process. *J. Biochem.* 125:277–284.

Ionov, R., A. ElAbed, A. Angelova, M. Goldmann, and P. Peretti. 2000. Asymmetrical ion-channel model inferred from two-dimensional crystallization of a peptide antibiotic. *Biophys. J.* 78:3026–3035.

Kem, W. R. 1988. Sea anemone toxin: structure and action. *In* The Biology of Nematocysts. D. A. Hessinger and H. M. Lenhoff, editors. Academic Press, San Diego. 375–405.

Lacy, D. B., and R. C. Stevens. 1998. Unraveling the structures and modes of action of bacterial toxins. *Curr. Opin. Struct. Biol.* 8:778–784.

Lakowicz, J. R. 1983. Principles of Fluorescence Spectroscopy. Plenum Press, NY.

Langner, M., and K. Kubica. 1999. The electrostatics of lipid surfaces. *Chem. Phys. Lipids.* 101:3–35.

Lanio, M. E., V. Morera, C. Alvarez, M. Tejuca, T. Gomez, I. F. Pazos, V. Besada, D. Martinez, V. Huerta, G. Padron, and M. A. Chavez. 2001. Purification and characterization of two hemolysins from *Stichodactyla helianthus*. *Toxicon.* 39:187–194.

Lesieur, C., B. Vécsey-Semjén, L. Abrami, M. Fivaz, and F. G. van der Goot. 1997. Membrane insertion: the strategies of toxins (Review). *Mol. Membr. Biol.* 14:45–64.

Lewis, R. N. A. H., and R. N. McElhaney. 2000. Surface charge markedly attenuates the nonlamellar phase-forming propensities of lipid bilayer membranes: calorimetric and P-31-nuclear magnetic resonance studies of mixtures of cationic, anionic, and zwitterionic lipids. *Biophys. J.* 79:1455–1464.

Li, J., P. A. Koni, and D. J. Ellar. 1996. Structure of the mosquitocidal delta-endotoxin CytB from *Bacillus thuringiensis* sp. *kyushuensis* and implications for membrane pore formation. *J. Mol. Biol.* 257:129–152.

MacDonald, R. C., R. I. MacDonald, B. P. M. Menco, K. Takeshita, N. K. Subbarao, and L. Hu. 1991. Small-volume extrusion apparatus for preparation of large, unilamellar vesicles. *Biochim. Biophys. Acta.* 1061: 297–303.

Macek, P. 1997. Equinatoxins (*Actinia equina* L., sea anemone). *In* Guidebook to Protein Toxins and their Use in Cell Biology. R. Rappuoli and C. Montecucco, editors. Oxford University Press, Oxford. 241–242.

Macek, P., G. Belmonte, C. Pederzolli, and G. Menestrina. 1994. Mechanism of action of equinatoxin II, a cytolysin from the sea anemone *Actinia equina* L. belonging to the family of actinoporins. *Toxicology.* 87:205–227.

Macek, P., M. Zecchini, C. Pederzolli, M. Dalla Serra, and G. Menestrina. 1995. Intrinsic tryptophan fluorescence of equinatoxin II, a pore-forming polypeptide from the sea anemone *Actinia equina* L., monitors its interaction with lipid membranes. *Eur. J. Biochem.* 234:329–335.

Marx, U., G. Lassmann, H. G. Holzhutter, D. Wustner, P. Muller, A. Hohlig, J. Kubelt, and A. Herrmann. 2000. Rapid flip-flop of phospholipids in endoplasmic reticulum membranes studied by a stopped-flow approach. *Biophys. J.* 78:2628–2640.

Matsuzaki, K. 1998. Magainins as paradigm for the mode of action of pore forming polypeptides. *Biochim. Biophys. Acta.* 1376:391–400.

Matsuzaki, K. 1999. Why and how are peptide-lipid interactions utilized for self-defense? Magainins and tachyplesins as archetypes. *Biochim. Biophys. Acta.* 1462:1–10.

Mayer, L. D., M. J. Hope, and P. R. Cullis. 1986. Vesicles of variable size produced by a rapid extrusion procedure. *Biochim. Biophys. Acta.* 858: 161–168.

Meinardi, E., M. Florin-Christensen, G. Paratcha, J. M. Azcurra, and J. Florin-Christensen. 1995. The molecular basis of the self/non self selectivity of a coelenterate toxin. *Biochem. Biophys. Res. Commun.* 216: 348–354.

Menestrina, G., V. Cabiaux, and M. Tejuca. 1999. Secondary structure of sea anemone cytolysins in soluble and membrane bound form by infrared spectroscopy. *Biochem. Biophys. Res. Commun.* 254:174–180.

Menestrina, G., S. Forti, and F. Gambale. 1989. Interaction of tetanus toxin with lipid vesicles. Effects of pH, surface charge and transmembrane potential on the kinetics of channel formation. *Biophys. J.* 55:393–405.

Op den Kamp, J. A. F. 1979. Lipid asymmetry in membranes. *Annu. Rev. Biochem.* 48:47–71.

Oren, Z., and Y. Shai. 1998. Mode of action of linear amphipathic alpha-helical antimicrobial peptides. *Biopolymers.* 47:451–463.

Panchal, R. G., E. Cusak, S. Cheley, and H. Bayley. 1996. Tumor protease-activated, pore-forming toxins from a combinatorial library. *Nature Biotech.* 14:852–856.

Pazos, I. F., C. Alvarez, M. E. Lanio, D. Martinez, V. Morera, E. Lissi, and A. Campos. 1998. Modification of sticholysin II hemolytic activity by free radicals. *Toxicon.* 36:1383–1393.

Pecora, R. 1985. Dynamic Light Scattering. Plenum Press, New York.

Pederzolli, C., G. Belmonte, M. Dalla Serra, P. Macek, and G. Menestrina. 1995. Biochemical and cytotoxic properties of conjugates of transferrin with equinatoxin II, a cytolysin from a sea anemone. *Bioconjugate Chem.* 6:166–173.

Rietveld, A., and K. Simons. 1998. The differential miscibility of lipids as the basis for the formation of functional membrane rafts. *Biochim. Biophys. Acta.* 1376:467–479.

Russo, M. J., H. Bayley, and M. Toner. 1997. Reversible permeabilization of plasma membranes with an engineered switchable pore. *Nature Biotech.* 15:282.

Santos, N. C., and M. A. R. B. Castanho. 1996. Teaching light scattering spectroscopy: the dimension and shape of tobacco mosaic virus. *Biophys. J.* 71:1641–1650.

Schneider, E., C. W. M. Haest, G. Plasa, and B. Deuticke. 1986. Bacterial cytotoxins, amphotericin B and local anesthetics enhance transbilayer

mobility of phospholipids in erythrocyte membranes. Consequences for phospholipid asymmetry. *Biochim. Biophys. Acta.* 855:325–336.

Seddon, J. M. 1990. Structure of the inverted hexagonal (H_{II}) phase, and non-lamellar phase transitions of lipids. *Biochim. Biophys. Acta.* 1031: 1–69.

Seddon, J. M., R. D. Kaye, and D. Marsh. 1983. Induction of the lamellar-inverted hexagonal phase transition in cardiolipin by protons and divalent cations. *Biochim. Biophys. Acta.* 734:347–352.

Staudegger, E., E. J. Prenner, M. Kriechbaum, G. Degovics, R. N. A. H. Lewis, R. N. McElhaney, and K. Lohner. 2000. X-ray studies on the interaction of the antimicrobial peptide gramicidin S with microbial lipid extracts: evidence for cubic phase formation. *Biochim. Biophys. Acta.* 1468:213–230.

Tejuca, M., G. Anderluh, P. Macek, C. Alvarez, M. E. Lanio, R. Marcet, D. Torres, J. Sarracent, M. Dalla Serra, and G. Menestrina. 1999. Antiparasite activity of sea anemone cytolysins on *Giardia duodenalis* and specific targeting with anti-*Giardia* antibodies. *Int. J. Parasitol.* 29:489–498.

Tejuca, M., M. Dalla Serra, M. Ferreras, M. E. Lanio, and G. Menestrina. 1996. The mechanism of membrane permeabilization by sticholysin I, a cytolysin isolated from the venom of the sea anemone *Stichodactyla helianthus. Biochemistry.* 35:14947–14957.

Turk, T. 1991. Cytolytic toxins from sea anemones. *J. Toxicol. -Toxin Rev.* 10:223–262.

Varanda, A., and A. Finkelstein. 1980. Ion and non electrolyte permeability properties of channels formed in planar lipid bilayer membranes by the cytolytic toxin from the sea anemone, *Stoichactis helianthus. J. Membr. Biol.* 55:203–211.

Yang, L., T. M. Weiss, R. I. Lehrer, and H. W. Huang. 2000. Crystallization of antimicrobial pores in membranes: magainin and protegrin. *Biophys. J.* 79:2002–2009.